Revista Brasileira de Cartografia
ISSN 1808-0936 | https://doi.org/10.14393/revbrascartogr
Sociedade Brasileira de Cartografia, Geodésia, Fotogrametria e Sensoriamento Remoto

Burned area mapping in Different Data Products for the Southwest of the Brazilian Amazon

Mapeamento de Queimadas em Diferentes Produtos de Área Queimada para o Sudoeste da Amazonia Brasileira

Débora Joana Dutra [1*], Philip Martin Fearnside [2], Aurora Miho Yanai [2], Paulo Maurício Lima de Alencastro Graça [2], Ricardo Dalagnol [3,4], Ana Carolina Moreira Pessôa [5], Beatriz Figueiredo Cabral [1], Chantelle Burton [6], Christopher Jones [6], Richard Betts [6], Poliana Domingos Ferro [7], Daniel Alves Braga [8], Luiz Eduardo Oliveira e Cruz de Aragão [7] and Liana Oighenstein Anderson [1]

1 National Center for Monitoring and Early Warning of Natural Disasters, São José dos Campos, Brazil. ddutra.ambiental@gmail.com, beatriz.figueiredocabral@gmail.com and liana.anderson@cemaden.gov.br
ORCID: https://orcid.org/0000-0003-3748-5622, https://orcid.org/0000-0002-7130-9385 and https://orcid.org/0000-0001-9545-5136
2 National Institute for Research in Amazonia, Manaus, Brazil. pmfearn@inpa.gov.br, yanai@inpa.gov.br and pmlag@inpa.gov.br
ORCID: https://orcid.org/0000-0003-3672-9082, https://orcid.org/0000-0003-2128-9547 and https://orcid.org/0000-0003-2173-1518
3 Jet Propulsion Laboratory, Los Angeles, United States. dalagnol@ucla.edu
ORCID: https://orcid.org/0000-0002-7151-8697
4 University of California, Los Angeles, United States.
5 Amazon Environmental Research Institute, Brasília, Brazil. acmoreirapessoa@gmail.com
ORCID: https://orcid.org/0000-0003-3285-8047
6 Met Office Hadley Centre, Exeter, UK. chantelle.burton@metoffice.gov.uk, chris.d.jones@metoffice.gov.uk and richard.betts@metoffice.gov.uk
ORCID: https://orcid.org/0000-0003-0201-5727, https://orcid.org /0000-0002-7141-9285 and https://orcid.org/0000-0002-4929-0307
7 National Institute for Space Research, São José dos Campos, Brazil. poliana.ferro@inpe.br and luiz.aragao@inpe.br
ORCID: https://orcid.org/0000-0001-7702-077X and https://orcid.org/0000-0002-4134-6708
8 Federal University of Santa Catarina, Florianópolis, Brazil. danielalvezbraga@gmail.com
ORCID: https://orcid.org/0000-0002-5170-1902

*Author to whom correspondence should be addressed.

Recebido: 02.2023 | Aceito: 10.2023

Abstract: Fires affect the Amazon rainforest and cause various socio-environmental problems. Analyses of forest fire dynamics supporting actions to combat and prevent forest fires. However, many studies have reported discrepancies in the quantification of fire, especially in the tropics. We evaluated four operational products for estimating burned areas (MAPBIOMAS, MCD64A1, GABAM, and GWIS) in a part of the southwestern Brazilian Amazon. We used the year 2019 as a reference to assess the relative performance of each product through stratification by forest and non-forest areas. Statistical (Kolmogorov–Smirnov test) and geospatial analyses were performed using fuzzy similarity analysis and mapping of burned areas for forest and non-forest classes. The four products showed a divergence of up to 90.6% in the total area burned. MAPBIOMAS was the product with the largest area burned (3379 km²), and MCD64A1 detected the smallest area (325 km²). MAPBIOMAS and GABAM generally overestimates burn scars in forest areas compared to MCD64A1 and GWIS. Factors that influence the mapping of burned areas include cloud shadow, the spatial resolution of sensors, and external noises (drought and decomposition of bamboo forests). We highlight the importance of field validation when mapping imagery to differentiate the truly burned areas from targets with similar spectral behavior.
Keywords: Forest fire. Burned area. Land use cover change. Geospatial analyses.

Resumo: Os incêndios afetam a floresta amazônica e causam diversos problemas socioambientais. O monitoramento da dinâmica dos incêndios florestais é importante para apoiar tanto ações de combate quanto sua

prevenção. No entanto, muitos estudos relataram discrepâncias na quantificação de queimadas, especialmente nos trópicos. Neste estudo, avaliamos quatro produtos operacionais de áreas queimadas (MAPBIOMAS, MCD64A1, GABAM e GWIS) em uma área localizada no sudoeste da Amazônia brasileira. O ano de 2019 foi usado como referência para avaliar o desempenho relativo de cada produto por meio da estratificação por áreas florestais e não florestais. Foram feitas análises estatísticas utilizando o teste de Kolmogorov– Smirnov, e geoespaciais, por meio da análise de similaridade Fuzzy e mapeamento de área queimada para classe floresta e não floresta. Os quatro produtos apresentaram divergência de até 90,6% quanto à extensão de área total queimada. O MAPBIOMAS foi o produto que apresentou a maior extensão de área queimada (3.379 km²). Inversamente, o MCD64A1 foi o que detectou a menor extensão (325 km²). Além disso, identificou-se que o MAPBIOMAS e GABAM geralmente superestimam cicatrizes de queimada nas áreas florestais quando comparado com o MCD64A1 e GWIS. Existem fatores que influenciam no mapeamento de áreas queimadas, sendo eles a sombra de nuvem, resolução espacial dos sensores e ruídos externos, como a mortalidade de manchas de bambo no dossel florestal. Sugerimos que o uso de imagens deve ser acompanhado de análises de campo e integradas com imagens de reflectância da superfície multitemporispara avaliar as cicatrizes de áreas queimadas de alvos semelhantes espectralmente.
Palavras-chave: Incêndio florestal. Área queimada. Mudança na cobertura do solo. Análises geoespaciais.

1 INTRODUCTION

Human activities, such as deforestation and forest degradation, are the main cause of land-use transformations in the Amazon rainforest (BERLINCK; BATISTA, 2020; LAPOLA *et al.*, 2023), which has made the area more susceptible to fire events (FEARNSIDE, 2008; SILVEIRA *et al.*, 2022). From 2001 to 2018, 122,624 km² of Amazon Forest area was burned, representing a 1.8% of the forest area (ALENCAR *et al.*, 2022; LAPOLA *et al.*, 2023; SILVEIRA *et al.*, 2022). Increases in deforestation and forest degradation driven by fire have been frequent in the Amazon Forest (DUTRA *et al.*, 2023) and cause negative impacts on the hydrological (LEITE-FILHO *et al.*, 2021) and carbon cycles (ARAGÃO *et al.*, 2018; LEITE-FILHO, ARGEMIRO TEIXEIRA *et al.*, 2021; MARASENI *et al.*, 2016; PRENTICE *et al.*, 2011; SHAKESBY; DOERR, 2006), as well as harming human health (CAMPANHARO *et al.*, 2022). Fire events cause loss of biodiversity (MATAVELI; CHAVES; *et al.*, 2021; MATAVELI; DE OLIVEIRA; *et al.*, 2021; MATAVELI*t al.*, 2017; ROSSI *et al.*, 2022), economic losses (CAMPANHARO, WESLEY A. *et al.*, 2019; DE MENDONÇA *et al.*, 2004), carbon emissions (ARAGÃO *et al.*, 2018; LAPOLA *et al.*, 2023). These impacts are amplified by climate change due to interactions with extreme droughts (ARAGÃO *et al.*, 2018; ARAGÃO; SILVA-JUNIOR; ANDERSON, 2020; CARVALHO *et al.*, 2021; GATTI *et al.*, 2021; SILVA JUNIOR *et al.*, 2019). Because tropical forests are important global climate regulators and providers of environmental services, it is crucial to develop actions to monitor fire-related activities to support measures for preventing and mitigating environmental impacts (BARLOW *et al.*, 2023; DE ANDRADE *et al.*, 2020; MATAVELI; CHAVES; *et al.*, 2021; MATAVELI; DE OLIVEIRA; *et al.*, 2021).

Remote sensing techniques have allowed the development of methodological approaches to detect and monitor burned areas in the Amazon Forest (ANDERSON *et al.*, 2015; GIGLIO *et al.*, 2018; PENHA *et al.*, 2020; SHIMABUKURO *et al.*, 2015). These methodologies have specificities that suit different purposes. For instance, it is possible to identify differences in the spatial distribution, time, size, and frequency of burned areas using different data products (LONG *et al.*, 2019; MOUILLOT *et al.*, 2014; PESSÔA *et al.*, 2020). Nevertheless, divergences among maps create the need to use a tool to compare burned-area estimates (PESSÔA *et al.*, 2020). This process allows evaluation of the mapping according to relative performance, especially when there are no field validation points in the area (HUMBER *et al.*, 2019; PADILLA *et al.*, 2015).

The different burned area products have a variety of limitations, and intercomparisons should be used as a complement to the product validation process (PESSÔA *et al.*, 2020), since any mapping methodology only provides an approximation of the real conditions (HUMBER *et al.*, 2019). Given this limitation, an intercomparison analysis helps in understanding the advantages and disadvantages of the

products for different purposes. The analyses must be carried out according to the product specifications and be balanced in selecting data to be included in the analysis, in view of the final objective (BOSCHETTI, L. *et al.*, 2020; BOSCHETTI, LUIGI *et al.*, 2019; PESSÔA *et al.*, 2020). Although several studies have assessed differences in the results of burned-area products (ANDERSON *et al.*, 2015; PENHA *et al.*, 2020; PESSÔA *et al.*, 2020), their intercomparison suggests that performance is spatially heterogeneous. A prior area evaluation should therefore be carried out before selecting a product for operational usage for guiding public policies and action (PESSÔA *et al.*, 2020).

This paper is an extended version of Dutra *et al.* (2022), presented at the XXIII Brazilian Symposium on GeoInformatics (GEOINFO, 2022). Here we assessed four operational burned-area products (MAPBIOMAS, MCD64A1, GABAM, and GWIS) for the southwest Brazilian Amazon, a region increasingly threatened by fires (DUTRA *et al.*, 2023) and located adjacent to the arc of deforestation (DOMINGUES; BERMANN, 2012). The specific objectives were to evaluate the similarities and differences amongst operational burned-area products in forest and non-forest areas in a municipality located in the new arc of deforestation, in the southern portion of Amazonas state, and to analyze the spatial similarities and differences among the products.

2 MATERIALS AND METHODS

2.1 Study Area

The study area covered a total area of 40,777 km² and consisted of the municipality of Boca do Acre in Amazonas state plus a 25-km buffer around the municipality. The buffer area covers parts of the municipalities of Pauini (19.42%), Lábrea (5.42%), Acrelândia (1.91%), Senador Guiomard (16.16%), Porto Acre (79.01%), Bujari (28.18%), Sena Madureira (9.58%) and Manoel Urbano (13.68%) (Figure 1).

Figure 1 - Study area located in the municipality of Boca do Acre, state of Amazonas. Forest proportion in a grid of 5 × 5 km pixels extracted by the Amazon Forest Deforestation Calculation Program (PRODES) forest mask for 2019. This was used to select burned areas.

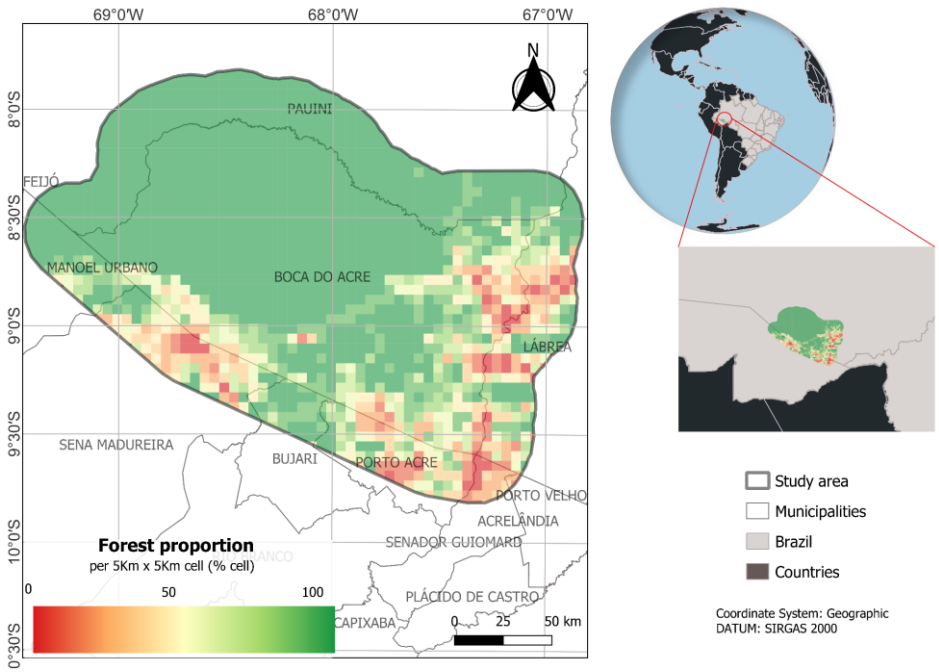

Source: Authors (2023).

There are seven indigenous territories in the study area: Camicua (583.9 km²), Igarapé Capana (1,293.0 km²), Inauini/Teuiní (2385.8 km²), Boca do Acre (261.7 km²), Apurinã (421.1 km²),

Peneri/Tacaquiri (487.0 km²), and Seruini/ Mariene (221.5 km²). There are also three conservation units (protected areas for biodiversity): Mapiá-Inauiní National Forest (3689.4 km²), Purus National Forest (1919.1 km²), and the Arapixi Extractive Reserve (1337.0 km²). This means that 30.9% of the study area corresponds to protected areas (indigenous lands and conservation units). According to PRODES data, in 2019 the region covered 33,335.80 km² of forest characterized as dense rainforest (Amazon Forest) (ASSIS *et al.*, 2019). There are also mosaics of oligotrophic woody vegetation (*campinarana*), and ecotone areas (BARNI *et al.*, 2015). The climate is classified as equatorial forest climate (Af) according to the Köppen classification (ALVARES *et al.*, 2013).

2.2 Burned-area data

We considered three global burned-area products: MCD64A1 (GIGLIO *et al.*, 2018), GABAM (LONG *et al.*, 2019), GWIS (BOSCHETTI, L. *et al.*, 2020), and one regional product: MAPBIOMAS Fogo, which covers Brazil (ALENCAR *et al.*, 2022; ARRUDA *et al.*, 2021) for the intercomparison of burned-area detection. MCD64A1 and GWIS use MOD14A1 data as inputs (i.e., MODIS C6 Terra/Aqua atmospherically corrected Level 2G daily surface reflectance and the C6 1-km Terra) and MYD14A1 (i.e., Aqua Level 3 daily active-fire products) (JUSTICE *et al.*, 2002). The detection method was produced by composite imagery summarizing persistent changes in the burn-sensitive vegetation index and using spatial and temporal active fire information to guide the statistical characterization of burn-related and non-burn-related change (GIGLIO *et al.*, 2018). GABAM uses Landsat imagery (Landsat 7, and 8) to validate the burned area mapping with reference data from other parts of the world (LONG *et al.*, 2019). MAPBIOMAS uses Landsat imagery (Landsat 5, 7, and 8) and a Deep Neural Network (DNN) model to detect and map burned areas in different Brazilian regions (ALENCAR *et al.*, 2022). All burned area products show annual data. The difference about the time series is the products used to create the burned areas. MCD64A1 has a temporal resolution of 1 to 2 days and 36 spectral bands, and LANDSAT has 16 days and 9 spectral bands.

The MCD64A1 and GWIS products have 500-m spatial resolution, while MAPBIOMAS and GABAM have 30-m spatial resolution (Table 1). The burned areas mapped for the year 2019 were selected for this analysis because this was the most recent year with mapping by all of the burned-area products. The GWIS products were discontinued in the year 2019.

Table 1- Specifications of the burned-area products.

Name	Spatial Resolution	Temporal Scale	Sensor	Scale
GABAM	30 m	1985-2019	TM/ ETM +/OLI	Global
GWIS	500 m	2001-2019	MODIS	Global
MAPBIOMAS	30 m	2000-2020	TM/ ETM +/OLI	National (Brazil)
MCD64A1	500 m	2000 - present	MODIS	Global

Source: Authors (2023).

2.3 Analysis

2.3.1 GEOSPATIAL ANALYSIS

We created a regular grid with a cell size of 5 × 5 km for the intercomparison between burned-area products. The proportion of the burned area detected by each product was calculated for each 5 × 5 km grid cell. We then calculated the total burned area estimated by each product, stratifying forest/non-forest land cover. For this purpose, the PRODES land-cover data from 2019 (ASSIS *et al.*, 2019) were used to separate the landscape into forest and non-forest (i.e., deforestation and non-forest vegetation). To create the land-use classes, we removed the hydrographic area by application of the water mask by Pekel *et al.* (2016) in the PRODES land-use map. Data processing was conducted using functions from the 'gdal' library) in

QGIS 3.22.6 software (QGIS, 2019), as well as the 'rgeos' package (BIVAND.; RUNDEL, 2018) in RStudio statistical software (R CORE TEAM, 2021).

2.3.2 STATISTICAL ANALYSIS

To analyze the significance of differences between the burned-area products, we first applied the non-parametric Kolmogorov–Smirnov two-sample test (SMIRNOV, 1939) for pair-wise comparisons to the fraction (from the 5 × 5 km cells) amongst the products, resulting in six total comparisons. We used the 'raster' package (HIJMANS, 2017) of RStudio software (R CORE TEAM, 2021) to process the data in the grid. We applied the conditional repeating structures in Bootstrap to create 10,000 interactions of 10% of the total cells. In this process, we applied randomly selected replacements in each execution of the conditional structure. The results are the mean and standard deviation of the 10,000 p-values resulting from the interactions.

To assess the spatial dependence, we employed a modeling approach using DINAMICA EGO 6 (LEITE-FILHO *et al.*, 2020; SOARES-FILHO *et al.*, 2004). We included a two-by-two statistical comparison using the fuzzy numerical method implemented in the "calc reciprocal similarity map" functor with a constant decay function (DINAMICA EGO TEAM, 2020). These analyses used the spatial similarity between pairs of pixels in two numerical maps, using the neighborhood (window size of 3 lines by 3 columns) to calculate the similarity of each pixel (DINAMICA EGO TEAM, 2020). This window size was chosen to get the most precision from the similarity analysis for use in the Dinamica EGO system. The value interval of results is between 0 (fully distinct) and 1 (fully identical).

3 RESULTS

3.1 Burned-Area Detection

We detected a total burned area of 7167 km² (summed considering the overlap between the products) in 2019. Of this total, 264 km² (3.69%) was in the forest area and 6903 km² (96.31%) was in the non-forest area (Figure 2). In forest areas, GWIS and MCD64A1 detected larger burned area extents: 90 km² (33.6%) and 100 km² (38.6%), respectively. In non-forest areas, GABAM and MAPBIOMAS detected larger extents: 3111 km² (46.5%) and 3338 km² (49.9%), respectively.

Figure 2 - Percentage of the total burned area detected by each product that is in forest and non-forest. (a) Percentage of the area classified as burned by each product in the forest area, and (b) Percentage of the area classified as burned by each product in the non-forest area.

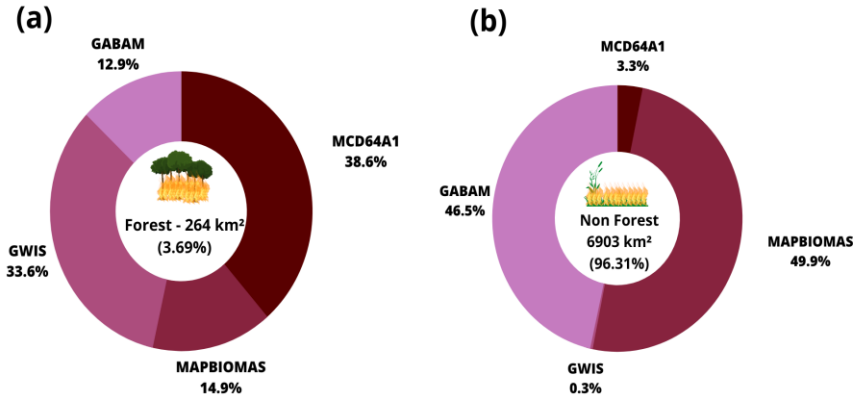

Source: Authors (2023).

Our results show the greatest difference between MAPBIOMAS and MCD64A1, where in the study

area as a whole (both forest and non-forest area) MCD64A1 mapped 3062 km² of burned area, or 90.6% less than the area mapped by MAPBIOMAS. In the non-forest area, MAPBIOMAS detected 3338 km² of burned area, or 30.4% more than the area detected by MCD64A1, while in the forest area MAPBIOMAS detected 60 km², or 30.4% less than the area detected by MCD64A1 (Figure 3). Two groups of products produced similar results: GWIS/MCD64A1 and GABAM/ MAPBIOMAS. MCD64A1 detected 8 km², or 2.46% less total area burned than GWIS, but detected the most burned area in the forest class (100 km²) and smaller areas in the non-forest class (29 km²). MAPBIOMAS detected 234 km² of total burned area, or 6.9% more than GABAM, which detected 228 km² (8%) in non-forest areas and 5 km² (8%) in forest areas. All product combinations showed significant differences at the 5% significance level ($p < 0.05$, Table 2), except for the GWIS and MCD64A1 combination ($p = 0.0594$).

Figure 3 - Total burned area mapped by GABAM, GWIS, MAPBIOMAS, MCD64A1, and percentage of the total area in the forest and non-forest classes that was burned.

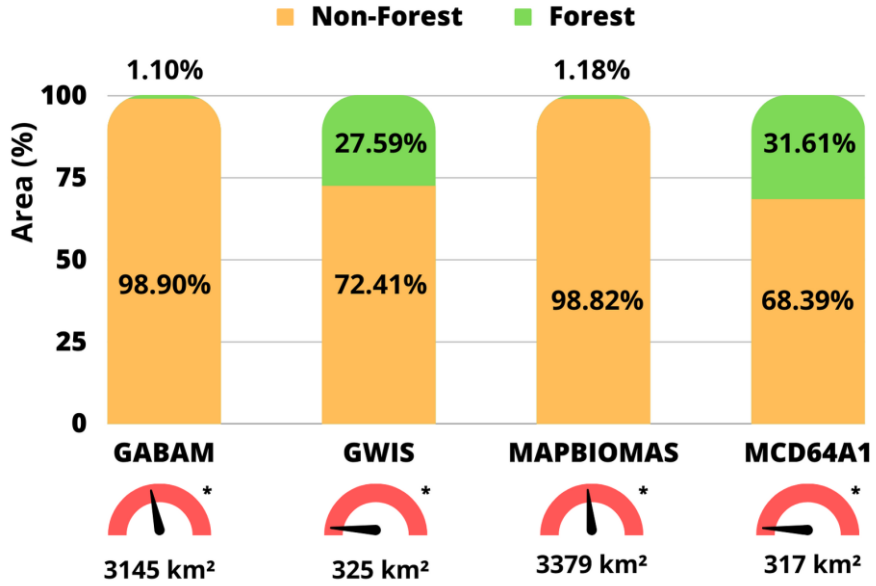

Source: Authors (2023).

Table 2 - Means and standard deviations of p-values resulted from 10,000 iterations of Kolmogorov-Smirnov two-sample tests, randomly selecting different samples of 10% of the total number of 5 × 5 l, (25 km²) grid cells.

Mean				
	GABAM			
GABAM	-	GWIS		
GWIS	6.97E-05	-	MAPBIOMAS	
MAPBIOMAS	3.22E-05	2.40E-08	-	MCD64A1
MCD64A1	1.04E-04	5.94E-01	3.13E-08	-
Sd				
	GABAM			
GABAM	-	GWIS		
GWIS	2.96E-04	-	MAPBIOMAS	
MAPBIOMAS	6.24E-05	5.27E-07	-	MCD64A1
MCD64A1	3.18E-04	2.91E-01	1.67E-07	-

Source: Authors (2023).

3.2 Mapping Differences

We observed that MAPBIOMAS had low similarity with other products (similarity index close to

0.5) (Figure 4). These results are associated with the MAPBIOMAS showing the largest mapped extent of burned area in comparison with GWIS and MCD64A1 decreasing the spatial similarity between them. In contrast, GABAM, GWIS, and MCD64A1, presented higher similarity (≥ 0.84) due to the lower extent of the burned area they mapped and due to similarity in the spatial distribution of burned pixel proportions, which makes them more likely to be similar.

Figure 4 - Overall similarity for each burned-area product comparison pair, considering the whole study area.

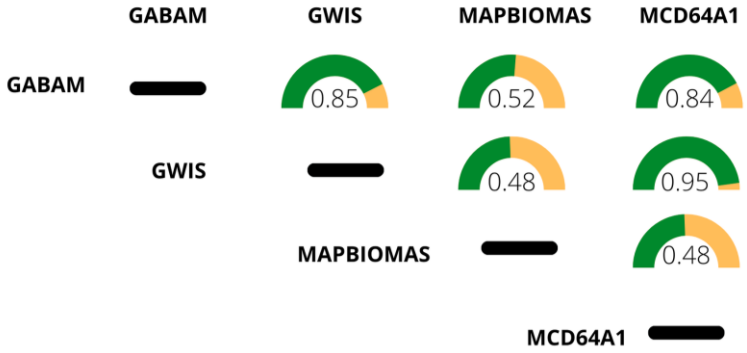

* The symbol in green represents the similarity performance on a scale of 0 to 1. In yellow, it is the difference between the similarity value and the maximum value (1)

Source: Authors (2023).

When inspecting the spatial patterns of burned areas across the study area, we observed that MAPBIOMAS was the only data product that mapped the majority of the central and northwestern portion of the study area. These areas were mapped with low burned area proportion (0 to 5%). In addition, in the southern and eastern portions of the study area, MAPBIOMAS identified a higher proportion of burned areas (> 20% of the grid cells) than did the other products (Figure 5). GABAM also found more widespread burned areas across the southern and eastern areas but with a much smaller proportion of burned areas (<5%). GWIS and MCD64A1 showed a very similar spatial pattern and similar burned area proportions.

Figure 5 – Burned-area spatialization in a 5 × 5 km regular grid. Each grid pixel contains the proportion of burned cells indicated by the color gradient.

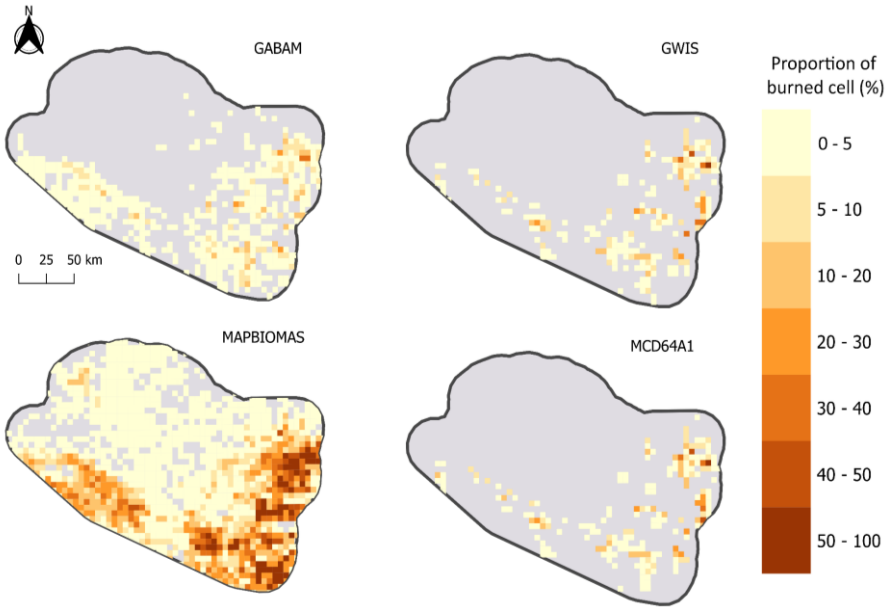

Source: Authors (2023).

Only 24% of the cells across the study area showed detections by all four data products (white cells in Figure 6). These cells were 22% covered by non-forest sites. Moreover, 42% of cells had burned areas mapped only by MAPBIOMAS data. These cells corresponded to 100% of the cells that had a part of the cell in the forest area. The remaining products only mapped burned cells with more than 1% of the cell burned. GABAM and MAPBIOMAS presented large areas of intersection, representing 43% of the total burned cells in the southern and eastern portions of the study area (Figure 6a).

Figure 6 - Confusion maps considering (a) the GABAM, MCD64A1, and MAPBIOMAS burned-area products, and (b) the GWIS, MCD64A1, and MAPBIOMAS burned-area products.

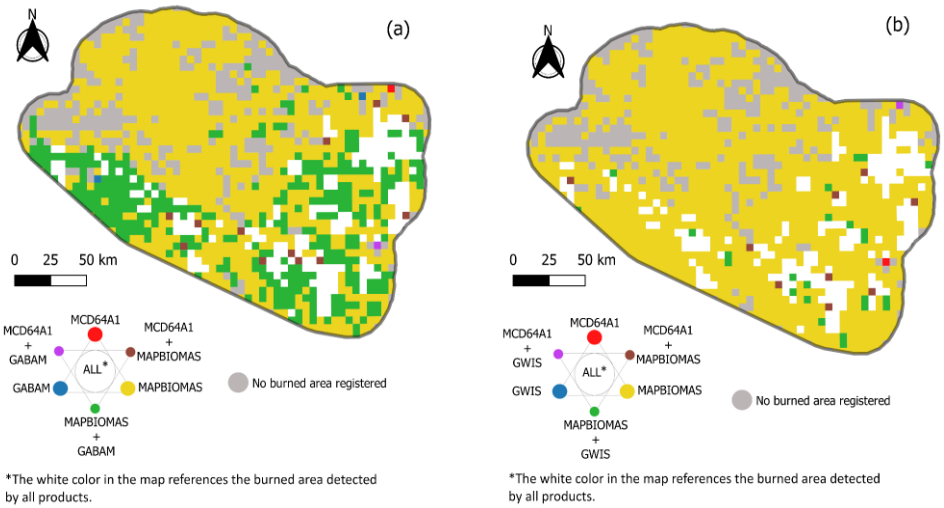

Source: DUTRA et al. (2022).

4 DISCUSSION

We identified two similar groups of data products associated with the type of satellite data source GWIS/MCD64A1 from MODIS (500 m) and GABAM/MAPBIOMAS from Landsat (30 m). The MCD64A1 product showed a total burned area (forest + non-forest) 2.46% to 90.61% lower than the other products we analyzed. However, this product detected the most burned area in forests: 10.51% to 65.47% more than the other products. Some studies have shown that MODIS data underestimate burned area by approximately 25% as compared to Landsat data (MORTON *et al.*, 2011; PESSÔA *et al.*, 2020; ROY; BOSCHETTI, 2009; SHIMABUKURO *et al.*, 2015), mainly due to its coarse spatial resolution. Thus, the estimated burned area using Landsat data was expected to be greater than by MODIS (SHIMABUKURO *et al.*, 2015). At the same time, the increased detection of MODIS over forested areas could be merely due to fires located in deforested areas that are close to forests borders because the 500-m MODIS pixel size can encompass both deforested and forest areas in the same pixel. The temporal resolution of Landsat data (used by GABAM and MAPBIOMAS) is relatively coarse (16 days), but the spatial resolution in the optical spectrum (30 m) is much higher than MODIS. The higher spatial resolution of Landsat allows improved definition of the boundaries of burned areas because these features avoid the mixture of burned and unburned patches in the same pixel (ARRUDA *et al.*, 2021; LONG *et al.*, 2019).

Limitations in the data analysis include the differing characteristics of the satellite sensors, such as spatial and temporal resolution, and the algorithms employed to detect the burned areas (PESSÔA *et al.*, 2020). However, the high temporal resolution of MODIS data (used for MCD64A1 and GWIS), allows for greater data acquisition and less interference from clouds (ALONSO-CANAS; CHUVIECO, 2015; PESSÔA *et al.*, 2020). This process increases the chances for the burn date to be accurately identified (BUSH *et al.*, 2008). Thus, the temporal frequency of MODIS data allows for a better identification of the time elapsed since burning and the speed at which vegetation regenerates after the fire (GIGLIO *et al.*,

2018). These are important factors for monitoring in tropical regions because the higher temporal frequency minimizes the effect of cloud cover and climatic conditions.

We identified MAPBIOMAS and GABAM (Landsat data) as generally overestimating burn scars, especially in forest areas, when compared to MCD64A1 and GWIS (MODIS data). However, burned area is underestimated in non-forest regions with products that use MODIS data as a reference. MAPBIOMAS and GABAM data registered an increase of 93% to 94% in the burned area mapping compared to MCD64A1 and GWIS, respectively. These differences can be associated with the spatial resolution of the data sources (LONG *et al.*, 2019). Another factor that causes errors in burned area detection in the southwest Amazon is the bamboo-dominated forests that naturally occur in this region (DE CARVALHO *et al.*, 2013; SILVA *et al.*, 2021) . After ~28 years of the bamboo life cycle, they flower and die in large groups, causing an accumulation of dry biomass in the forest canopy, which then causes the appearance of large patches with dark colors when observing optical imagery such as that from Landsat and MODIS (DALAGNOL *et al.*, 2018). It has been suggested that the increase in dry biomass could contribute to igniting large fires, but 18 years of remote sensing data analysis has not confirmed this hypothesis, except for drought years (DALAGNOL *et al.*, 2018). Therefore, the MAPBIOMAS method may be detecting part of these large-scale bamboo mortality events as burned areas. The developers of the method mentioned in a personal communication that this region lacks sampling data and that this issue should be improved in future versions.

While MAPBIOMAS and GABAM (the two datasets based on Landsat data at 30-m resolution) found approximately the same number of burned areas, they differed in terms of the size of the detections. The MAPBIOMAS regional product registered 11 times more burned area with small proportions (< 1.25 km² in cell grid proportion) when compared to the GABAM global product. According to the developers of GABAM (LONG *et al.*, 2019), the overestimated values with the use of Landsat data can be associated with temporal resolution and cloud shadow contamination (LONG *et al.*, 2019). This process is associated with a mapping limitation in tropical regions, where cloud cover is persistent and vegetation recovery is quick. Thus, we observed that overestimation by MAPBIOMAS and GABAM is associated with the detection of false positives, mainly in forest areas.

Burned-area grouping was different between the products, and the results showed specific spatial patterns. Ferro *et al.*, (2023) demonstrated with CBERS 4 and CBERS 4A data that the spatial pattern is better when the burned-area values are smaller. In this process, the overestimation or underestimation of the burned area found in our results showed how the spatial pattern can behave differently according to the mapping technique applied. Noise in this process was responsible for the differences between the scattered similarities of the comparison results. Some studies suggest the application of the shadow fraction imaging technique to highlight the burned areas and facilitate the image classification process (ANDERSON *et al.*, 2015; FERRO *et al.*, 2023; SHIMABUKURO *et al.*, 2020; SHIMABUKURO; SMITH, 1991). The combination of data from different sensors and the application of this technique avoids omission and commission errors in burned areas (FERRO *et al.*, 2023).

Studies using lower-resolution products, such as MCD64A1 and GWIS, demonstrate that they are unable to adequately detect small fires (< 100 ha) (RODRIGUES *et al.*, 2019), which can cause the burned area to be underestimated (GIGLIO *et al.*, 2018; JUSTICE *et al.*, 2002). Despite MCD64A1 presenting a significantly lower detection of small burns (< 100 ha) than other products (CHUVIECO *et al.*, 2018; JUSTICE *et al.*, 2002; PESSÔA *et al.*, 2020), we found underestimates of the burned area by 89.90% to 90.61% as compared to the higher-resolution products (30 m). Therefore, GABAM and MAPBIOMAS detect small burned areas better, showing small burn proportions associated with small burned patches in the grid with 5 km × 5 km (25 km^2) pixels.

The methodologies applied for mapping burned areas are a factor that can influence the differences in the mapping of products with the same spatial resolution. The MCD64A1 uses a burn-sensitive vegetation index to create a dynamic threshold to produce the burned composite data (GIGLIO *et al.*, 2018).

Their differences from the GWIS are associated with the post-processing applied to the MCD64A1 product, grouping pixels through an algorithm of growth analysis of burned areas (BOSCHETTI *et al.*, 2020; GIGLIO *et al.*, 2018). This process increased by ~2.46% of the burned areas in the study region mapped by the GWIS than the MCD64A1. However, these products have limitations associated with low confidence in identifying burned areas in crop areas, which may further overestimate the burned areas in a given region (BOSCHETTI, L. *et al.*, 2020; GIGLIO *et al.*, 2018) .

Regarding mappings with machine learning systems, we observed that application of the Random Forest system to the GABAM data (LONG *et al.*, 2019) and of the Deep Neural Network to the MAPBIOMAS data (ALENCAR *et al.*, 2022; ARRUDA *et al.*, 2021) increased the detected burned area surfaces by ~90%. These processes allow mapping smaller areas when compared to analyses using image classifiers (LONG *et al.*, 2019). However, the automated algorithm system applied in Landsat images shows limitations associated with omission errors in the tropical zone. These errors stemmed from the rapid vegetation recovery of the surface and the difficulty of machine learning models in disassociating differences between bamboo areas and fires (ALENCAR *et al.*, 2022; ARRUDA *et al.*, 2021; DALAGNOL *et al.*, 2018; LONG *et al.*, 2019).

Our findings highlight that the use of a single burned-area data product may not be representative of the reality of the burned areas on the ground. One potential solution would be the combination of multiple single-burned data products into a multi-source burned area product (LEÃO *et al.*, 2022; PESSÔA *et al.*, 2020). The development of such a product allows an index of confidence to be created based on the number of detections amongst different products for the same area. This product would reduce false positives in detection and allow a more conservative and precise assessment of burned areas in tropical forests (LEÃO *et al.*, 2022). It is desirable to have an independent burned-area map that is produced with detail and human editing for a more comprehensive quantification of the operational product strengths and limitations. In the absence of a national product that does not require adjustment in the algorithm, the global products still prove to be reliable (within the highlighted limitations) for operationalization and analysis of socio-environmental losses related to tropical forest fires.

Burned-area products are useful for quantification of the extension area affected by fires, except for ecological consequences, such as forest mortality and heterogeneity or irregularity of burning associated with the behavior of fire in the environment (KEY; BENSON, 2006). In this sense, field validation help reduce overestimates and underestimations of burned area products. Regardless of the scale applied, mapping in the field faces significant difficulties associated with post-fire responses. This process requires large investments in equipment and labor, collection in areas with variability in the vegetation, selection of homogeneous land-use classes, adjustment of the analysis plots based on the spatial resolution of the sensor (e.g., considering Landsat data of 30 m, the areas must be at least 90 × 90 m), and establishment of sub-plots that never deviate in the field and that have good accuracy in georeferencing (KEY, 2004; KEY; BENSON, 2006). Another factor is the difficulty of access, i.e., a region may be at the bottom of rural properties requiring authorization for entry or may not be accessible by road. Furthermore, in the Amazon another difficulty in field mapping is associated with most forest fires occurring in the understory (ALENCAR *et al.*, 2022), which is expected to not be detected by optical sensors. Therefore, the extent of forest fires in the Amazon may be considered underestimated, regardless of the product used.

5 CONCLUSIONS

A comparison of burned-area products allowed us to analyze the influence of spatial resolution and methodologic creation in burned-area analyses at the regional scale. Considering the magnitude of difference, GWIS and MCD64A1 were the most similar products because they identified a smaller difference in the burned area compared to other products. The products that differed the most were MAPBIOMAS and MCD64A1, these burned-area mappings differing by 90.62%. Regarding land use, we

observed that the products with higher resolution (GABAM and MAPBIOMAS) showed smaller differences in burned-area mapping than the products with lower resolution (GWIS and MCD64A1). The reduction of these differences may be associated with machine-learning techniques in the detection processes of burned-area products.

Differences can be observed between products with the same origin. For the two products using Landsat 8, MAPBIOMAS identified a greater amount of burned area than GABAM and registered smaller burned polygons. Despite the greater area mapping of the burned area, MAPBIOMAS may have registered a greater interference from noise and the contribution of small polygons. Reference data, such as ground validation or higher-resolution images, would be necessary to further evaluate this. At the municipality (county) scale, the data from GABAM, GWIS, and MCD64A1 were the most similar for mapping the area burned, despite differences in spatial resolution.

For mapping on a regional scale, the global products showed better performance at a spatial resolution of 5 km than the national product (MAPBIOMAS). We observed that products required adjustment with data from the field, and filters to remove interference from noise generated by bamboo and cloud shadow.

Acknowledgments

This research was funded by the São Paulo State Research Support Foundation (FAPESP) grant numbers 2021/04019-4, 2020/08916-8, 2020/15230-5, Amazonas State Research Support Foundation (FAPEAM) grant number 0102016301000289/2021-33. DJD was funded by DS Bridge – Amazon Task Force 2023. LOA was funded by the National Council for Scientific and Technological Development (CNPq) grant number 314473/2020-3. ACMP was funded by FAPESP grant number 2022/09380-0 and CNPq grant number 140877/2018-5. PMF was funded by CNPq grant number 312450/2021-4 and FINEP/Rede CLIMA grant number 01.13.0353-00. PMLAG, PMF, and AMY were funded by FAPEAM grant number 01.02.016301.01073/2023-57. This work and its contributors (CB, CDJ, RB) were funded by the Met Office Climate Science for Service Partnership (CSSP) Brazil project which is supported by the Department for Science, Innovation & Technology (DSIT).

Authors contribution

This article was prepared based on the contributions of all authors. D.J.D. conceptualization, data curation, formal analysis, validation and writing (editing, review), P.MF. visualization, writing (editing, review) and conceptualization. A.M.Y. visualization, writing (editing, review) and conceptualization. P.M.L.A.G. visualization, writing (editing, review) and conceptualization. R.D. visualization, writing (editing, review) and conceptualization. A.C.M.P. viewing, writing (editing, reviewing). B.F.C. viewing, writing (editing, reviewing). C.B. visualization, writing (editing, review). C.J., R.B. viewing, writing (editing, reviewing). P.D.F. viewing, writing (editing, reviewing). D.A.B. viewing, writing (editing, reviewing). L.E.O.C.A. viewing, writing (editing, reviewing). L.O.A visualization, guidance, supervision, acquisition of funding, resources, conceptualization, methodology, writing (editing, review).

Conflict of Interest

The authors declare that there is no conflict of interest.

References

ALENCAR, A. A. C. *et al.* Long-term Landsat-based monthly burned area dataset for the Brazilian biomes

using deep learning. **Remote Sensing**, v. 4, n. 11 art. 2510, 2022. DOI: 10.3390/rs14112510

ALONSO-CANAS, I.; CHUVIECO, E. Global burned area mapping from ENVISAT-MERIS and MODIS active fire data. **Remote Sensing of Environment**, v. 163, p. 140–152, Jun. 2015. DOI: 10.1016/j.rse.2015.03.011

ALVARES, C. A. *et al.* Köppen's climate classification map for Brazil. **Meteorologische Zeitschrift**, v. 22, n. 6, p. 711–728, 1 Dec. 2013. DOI: 10.1127/0941-2948/2013/0507

ANDERSON, L. O. C. *et al.* Disentangling the contribution of multiple land covers to fire-mediated carbon emissions in Amazonia during the 2010 drought. **Global Biogeochemical Cycles**, v. 29, n. 10, p. 1739–1753, out. 2015. DOI: 10.1002/2014GB005008

ARAGÃO, L. E. O. C. *et al.* 21st Century drought-related fires counteract the decline of Amazon deforestation carbon emissions. **Nature Communications**, v. 9, n. 1, p. 1–12, 2018. DOI: 10.1038/s41467-017-02771-y

ARAGÃO, L. E. O. C. *et al.*. **O desafio do Brasil para conter o desmatamento e as queimadas na Amazônia durante a pandemia por COVID-19 em 2020: implicações ambientais, sociais e sua governança***,* 1., nº 1. São José dos Campos, 2020. DOI: 10.13140/RG.2.2.17256.49921

ARRUDA, V. L. S. *et al.* An alternative approach for mapping burn scars using Landsat imagery, Google Earth Engine, and deep learning in the Brazilian savanna. **Remote Sensing Applications: Society and Environment**, v. 22, art. 100472, 2021. DOI: 10.1016/j.rsase.2021.100472

ASSIS, L. F. F. G. *et al.* TerraBrasilis: A Spatial data analytics infrastructure for large-scale thematic mapping. **ISPRS International Journal of Geo-Information**, v. 8, n. 11, p. 513, 2019. DOI: 10.3390/ijgi8110513

BARLOW, J. *et al.* Clarifying Amazonia's burning crisis. **Global Change Biology**, v. 26, n. 2, p. 319–321, 15 Feb. 2020. DOI: 10.1111/gcb.14872

BARLOW, J. et al. **Transformando a Amazônia através de "arcos de restauração"**. Technical report. EMPRAPA. 2023.

BARNI, P. E. *et al.* Deforestation and forest fires in Roraima and their relationship with phytoclimatic regions in the northern Brazilian Amazon. **Environmental Management**, v. 55, n. 5, p. 1124–1138, 21 May 2015. DOI: 10.1007/s00267-015-0447-7

BERLINCK, C.; BATISTA, E. K. L. Good fire, bad fire: It depends on who burns. **Flora Morphology, Distribution. Functional. Ecology of Plants**, v. 268, art. 151610, 2020. DOI: 10.1016/j.flora.2020.151610

BIVAND, R.; RUNDEL, C. **Rgeos: Interface to Geometry Engine—Open Source ('GEOS')**. Available at: <https://rdrr.io/cran/rgeos/>. Accessed: 30 jun. 2021.

BOSCHETTI, L. *et al.* Global validation of the collection 6 MODIS burned area product. **Remote Sensing of Environment,** v. 235, n. November, art. 111490, 2019. DOI: 10.1016/j.rse.2019.111490

BOSCHETTI, L. *et al.* **GWIS national and sub-national fire activity data from the NASA MODIS Collection 6 Burned Area Product in Support of Policy Making, Carbon Inventories and Natural Resource Management,** 2020. Available at: <https://gwis.jrc.ec.europa.eu/apps/country.profile/downloads>. Accessed: 6 jun. 2021.

BURTON, C. *et al.* El Niño driven changes in global fire 2015/16. **Frontiers in Earth Science**, v. 8, 10 Jun. 2020. DOI: 10.3389/feart.2020.00199

BUSH, M. *et al.* Fire, climate change and biodiversity in Amazonia: A Late-Holocene perspective. **Philosophical Transactions of the Royal Society B: Biological Sciences**, v. 363, n. 1498, p. 1795–1802, 27 May 2008. DOI: 10.1098/rstb.2007.0014

CAMPANHARO W. A. *et al*. Translating Fire Impacts in Southwestern Amazonia into Economic Costs. **Remote Sensing**.9 v.11,n.7764, 2019. DOI: 10.3390/rs11070764

CAMPANHARO, W. A. *et al.* Hospitalization due to fire-induced pollution in the Brazilian Legal Amazon from 2005 to 2018. **Remote Sensing**, v. 14, n. 1, art. 69, 2022. DOI: 10.3390/rs14010069

CARVALHO, A. L. *et al*. Bamboo-dominated forests of the southwest Amazon: detection, spatial extent, life cycle length and flowering waves. **PloS one**, v. 8, n. 1, p. e54852, 2013. DOI: 10.1371/journal.pone.0054852

CARVALHO, N. S. *et al.* Spatio-temporal variation in dry season determines the Amazonian fire calendar. **Environmental Research Letters**, v. 16, n. 12, art. 125009, 2021. DOI: 10.1088/1748-9326/ac3aa3

CHUVIECO, E. *et al.* Generation and analysis of a new global burned area product based on MODIS 250 m reflectance bands and thermal anomalies. **Earth System Science Data**, v. 10, n. 4, p. 2015–2031, 2018. DOI: 10.5194/essd-10-2015-2018

DA SILVA, S. S. *et al.* Increasing bamboo dominance in southwestern Amazon forests following intensification of drought-mediated fires. **Forest Ecology and Management**, v. 490, p. 119139, 2021. DOI: 10.1016/j.foreco.2021.119139

DALAGNOL, R. *et al*. Life cycle of bamboo in the southwestern Amazon and its relation to fire events. Biogeosciences, v. 15(20), p.6087–6104, 2018. DOI: 10.5194/bg-15-6087-2018

DE ANDRADE, D. F. C. *et al.* Forest resilience to fire in eastern Amazon depends on the intensity of pre-fire disturbance. **Forest Ecology and Management**, v. 472, art. 118258, Sept. 2020. DOI: 10.1016/j.foreco.2020.118258

DE MENDONÇA, M. J. C. *et al.* The economic cost of the use of fire in the Amazon. **Ecological Economics**, v. 49, n. 1, p. 89–105, May 2004. DOI: 10.1016/j.ecolecon.2003.11.011

DINAMICA EGO TEAM. **Calc Reciprocal Similarity Map.** Available at: <https://csr.ufmg.br/dinamica/dokuwiki/doku.php?id=calc_reciprocal_similarity_map>. Accessed: 5 jul. 2021.

DOMINGUES, M S and BERMANN, C. O arco de desflorestamento na Amazônia: da pecuária à soja. **Ambiente & sociedade***,* v. 15, p. 1-22, 2012. DOI: 10.1590/S1414-753X2012000200002

DUTRA, D. J. *et al.* **Comparison of regional scale burned area products for southwestern Brazilian Amazonia**. 2022, São José dos Campos: GEOINFO 2022, 2022. p. 12.

DUTRA, D. J. *et al.* Fire dynamics in an emerging deforestation frontier in southwestern Amazonia, Brazil. **Fire,** v. 6, n. 1, p. 2, 21 Dec. 2023. DOI: https://doi.org/10.3390/fire6010002

FEARNSIDE, P. M. Amazon forest maintenance as a source of environmental services. *Anais da* **Academia Brasileira de Ciências**, v. 80, n. 1, p. 101–114, Mar. 2008.

FERRO, P D *et al.* Detecção de áreas queimadas baseado no modelo linear de mistura espectral aplicado em cubo de dados do CBERS-4 e CBERS -4A no oeste de Rondônia, Brasil. **Simpósio Brasileiro de Sensoriamento Remoto**. Florianópolis. 2023

GATTI, L. V. *et al*. Amazonia as a carbon source linked to deforestation and climate change. **Nature**, v. 595, n. 7867, p. 388-393, 2021. DOI: 10.1038/s41586-021-03629-6

GEOINFO. **GEOINFO**. Available at: <http://www.geoinfo.info/geoinfo2022/index.php>.

GIGLIO, L. *et al.* The Collection 6 MODIS burned area mapping algorithm and product. **Remote Sensing of Environment,** v. 217, n. July, p. 72–85, 2018. DOI: 10.1016/j.rse.2018.08.005

HIJMANS, R. J. **Raster: Geographic Data Analysis and Modeling**. Available at: <https://rdrr.io/cran/raster/>. Accessed: 30 jun. 2021.

HUMBER, M. L. *et al.* Spatial and temporal intercomparison of four global burned area products.

International Journal of Digital Earth, v. 12, n. 4, p. 460–484, 3 Apr. 2019. DOI: 10.1080/17538947.2018.1433727

JUSTICE, C. *et al.* The MODIS fire products. **Remote Sensing of Environment,** v. 83, n. 1–2, p. 244–262, Nov. 2002. DOI: 10.1016/S0034-4257(02)00076-7

KEY, C. H.; BENSON, N. C. Landscape assessment (LA). **FIREMON: Fire effects monitoring and inventory system**, 164, LA-1,2006.

KEY, C. H. Ecological and sampling constraints on defining landscape fire severity. **Fire Ecology**, v. 2, n. 2, p. 34-59, 2006.

LANGFORD, Z. *et al.* Wildfire mapping in interior Alaska using deep neural networks on imbalanced datasets. **IEEE International Conference on Data Mining Workshops, ICDMW,** v. 2018-Nov,, n. August 2019, p. 770–778, 2019. DOI: 10.1109/ICDMW.2018.00116

LAPOLA, D. M. *et al.* The drivers and impacts of Amazon Forest degradation. **Science**, 379(6630), eabp8622,2023. DOI: 10.1126/science.abp8622

LEITE-FILHO, A. T. *et al.* **Modeling Environmental Dynamics with Dinamica EGO.** Available at: <https://www.csr.ufmg.br/dinamica/dokuwiki/doku.php?id=guidebook_start>. Accessed: 5 jul. 2021b.

LEITE-FILHO, A T *et al.* Deforestation reduces rainfall and agricultural revenues in the Brazilian Amazon. **Nature Communications**, v. 12, n. 1, art 12, 2021a. DOI: 10.1038/s41467-021-22840-7

LEÃO, P H A *et al*. **Contribuição de produtos de área queimada na Amazônia Maranhense: proposta de avaliações combinadas**. In: Simpósio Brasileiro de Geoinformática, 23. (GEOINFO), 2022, On-line. São José dos Campos: INPE, 2022.

LONG, T. *et al.* 30-m resolution global annual burned area mapping based on Landsat images and Google Earth Engine. **Remote Sensing**, v. 11, n. 5, p. 1–30, 2019. DOI: 10.3390/rs11050489

MARASENI, T. N. *et al.* Savanna burning methodology for fire management and emissions reduction: a critical review of influencing factors. **Carbon Balance Manag**, v. 1, 2016. DOI: 10.1186/s13021-016-0067-4

MATAVELI, G. A. V. *et al.* Analysis of fire dynamics in the Brazilian savannas. **Natural Hazards and Earth System Sciences Discussions**, n. March, p. 1–27, 2017. DOI: 10.5194/nhess-2017-90, 2017

MATAVELI, G. A. V. *et al.* Relationship between biomass burning emissions and deforestation in Amazonia over the last two decades. **Forests,** v. 12, n. 9, p. 1–19, 2021a. DOI: 10.3390/f12091217

MATAVELI, G. A. V. *et al.* The emergence of a new deforestation hotspot in Amazonia. **Perspectives in Ecology and Conservation**, v. 19, n. 1, p. 33–36, 2021b. DOI: 10.1016/j.pecon.2021.01.002

MORTON, D. C. *et al.* Mapping canopy damage from understory fires in Amazon forests using annual time series of Landsat and MODIS data. **Remote Sensing of Environment**, v. 115, n. 7, p. 1706–1720, Jul. 2011. DOI: 10.1016/j.rse.2011.03.002

MOUILLOT, F. *et al.* Ten years of global burned area products from spaceborne remote sensing—A review: Analysis of user needs and recommendations for future developments. **International Journal of Applied Earth Observation and Geoinformation**, v. 26, p. 64–79, Feb. 2014. DOI: 10.1016/j.jag.2013.05.014

PADILLA, M. *et al.* Comparing the accuracies of remote sensing global burned area products using stratified random sampling and estimation. **Remote Sensing of Environment,** v. 160, p. 114–121, abr. 2015. DOI: 10.1016/j.rse.2015.01.005

PEKEL, J *et al*. Belward, High-resolution mapping of global surface water and its long-term changes. **Nature**, v. 540, p 418-422. 2016. DOI:10.1038/nature20584

PENHA, T. V. *et al.* Burned area detection in the Brazilian Amazon using spectral indices and GEOBIA. **Revista Brasileira de Cartografia**, v. 72, n. 2, p. 253–269, 2020. DOI: 10.14393/rbcv72n2-48726

PESSÔA, A. C. M. *et al.* Intercomparison of burned area products and its implication for carbon emission estimations in the Amazon. **Remote Sensing**, v. 12, n. 23, p. 3864, 25 Nov. 2020. DOI: 10.3390/rs12233864

PRENTICE, I. C. *et al.* Modeling fire and the terrestrial carbon balance. **Global Biogeochemical Cycles,** v. 25, n. 3, p. n/a-n/a, Sept. 2011. DOI: 10.1029/2010GB003906

QGIS. *QGIS* **Geographic Information System.** Available at: <https://qgis.org/pt_BR/site/>. Accessed: 6 jun. 2021.

R CORE TEAM. *R.* **A Language and Environment for Statistical Computing 2020.** Available at: <https://www.r-project.org/>. Accessed: 2 may 2021.

RODRIGUES, J. A. *et al.* How well do global burned area products represent fire patterns in the Brazilian Savannas biome? An accuracy assessment of the MCD64 collections. **International Journal of Applied Earth Observation and Geoinformation**, v. 78, p. 318–331, Jun. 2019. DOI: 10.1016/j.jag.2019.02.010

ROSSI, L. C. *et al*. Predation on artificial caterpillars following understorey fires in human-modified Amazonian forests. **Biotropica**, v. 54, n. 3, p. 754-763, 2022. DOI: 10.1111/btp.13097

ROSSI, L. C. **The effect of forest degradation on ecosystem services related to frugivory and insectivory promoted by birds and mammals in Amazonian forests.** Thesis. Universidade Estadual Paulista. 2022.

ROY, D. P.; BOSCHETTI, L. Southern Africa validation of the MODIS, L3JRC, and GlobCarbon burned-area products. **IEEE Transactions on Geoscience and Remote Sensing,** v. 47, n. 4, p. 1032–1044, Apr. 2009. DOI: 10.1109/TGRS.2008.2009000

SAFI, Y.; BOUROUMI, A. Prediction of forest fires using artificial neural networks. **Applied Mathematical Sciences**, v. 7, n. 5–8, p. 271–286, 2013.

SHAKESBY, R. A.; DOERR, S. H. Wildfire as a hydrological and geomorphological agent. **Earth-Sci. Rev.**, v. 74, p. 269–307, 2006. DOI: 10.1016/j.earscirev.2005.10.006

SHIMABUKURO, Y E et al. Mapping burned areas of Mato Grosso state Brazilian Amazon using multisensor datasets. **Remote Sensing**, v. 12, n. 22, p. 3827, 2020. DOI: 10.3390/rs12223827

SHIMABUKURO, Y. E. *et al.* Estimating burned area in Mato Grosso, Brazil, using an object-based classification method on a systematic sample of medium resolution satellite images. **IEEE Journal of Selected Topics in Applied Earth Observations and Remote Sensing,** v. 8, n. 9, p. 4502–4508, 2015. DOI: 10.1109/JSTARS.2015.2464097

SHIMABUKURO, Y. E. and SMIT, J. A. The least-squares mixing models to generate fraction images derived from remote sensing multispectral data. **IEEE Transactions on Geoscience and Remote Sensing**, v. 29, pp. 16–20, 1991. DOI: 10.1109/36.103288

SILVA JUNIOR, C. H. L. *et al.* Fire responses to the 2010 and 2015/2016 Amazonian droughts. **Frontiers in Earth Science**, v. 7, n. May, p. 1–16, 2019. DOI: 10.3389/feart.2019.00097

SILVEIRA, M. V. F. *et al.* Amazon fires in the 21st century: The year of 2020 in evidence. **Global Ecology and Biogeography,** n. September 2022. DOI: 10.1111/geb.13577

SMIRNOV, N. V. Estimate of deviation between empirical distribution functions in two independent samples. **Bull. Math. Univ. Moscow**, v. 2, p. 3–14, 1939.

SOARES-FILHO, B. *et al.* Simulating the response of land-cover changes to road paving and governance along a major Amazon highway: The Santarém-Cuiabá corridor. **Global Change Biology**, v. 10, n. 5,

p. 745–764, 2004. DOI: 10.1111/j.1529-8817.2003.00769.x

WARMERDAM, F. **The geospatial data abstraction library.** Open source approaches in spatial data handling, p. 87-104, 2008.

First author biography

Master's degree in Analysis and Modeling of Environmental Systems from UFMG, with a Bachelor's degree in Environmental and Sanitarist Engineering from CEFET-MG. Currently, she is a scholarship recipient at CEMADEN and a collaborator at the TREESlab of INPE, focusing on studies related to drought in hydrographic basins, wildfires, and forest degradation in the Amazon. She also served as a tutoring scholarship recipient at CEFET-MG, teaching geoprocessing and remote sensing. Additionally, she volunteered in a scientific initiation project, with an emphasis on analyzing environmental vulnerability in disasters involving tailings dams. She founded the Environmental Engineering and Entrepreneurship League (SUSTENTAR) at CEFET-MG and interned at FEAM, focusing on licensing, inspection, and monitoring of domestic and industrial effluents in Minas Gerais. She was awarded the Diamond League prize by the Estudar Foundation in 2015.